

See discussions, stats, and author profiles for this publication at: <https://www.researchgate.net/publication/257850465>

Graphene production by etching natural graphite single crystals in a plasma-chemical reactor based on beam-plasma discharge

Article *in* Doklady Physics · January 2012

Impact Factor: 0.6 · DOI: 10.1134/S1028335812010077

CITATIONS

3

READS

31

6 authors, including:



[Yu. I. Latyshev](#)

Russian Academy of Sciences

100 PUBLICATIONS 1,431 CITATIONS

[SEE PROFILE](#)



[Andrey P. Orlov](#)

Kotel'nikov Institute of Radioengineering an...

34 PUBLICATIONS 177 CITATIONS

[SEE PROFILE](#)



[V. V. Peskov](#)

Kotel'nikov Institute of Radioengineering an...

5 PUBLICATIONS 8 CITATIONS

[SEE PROFILE](#)



[Evgeniy Shustin](#)

Kotel'nikov Institute of Radioengineering an...

48 PUBLICATIONS 71 CITATIONS

[SEE PROFILE](#)

Graphene Production by Etching Natural Graphite Single Crystals in a Plasma-Chemical Reactor Based on Beam-Plasma Discharge

Yu. I. Latyshev, A. P. Orlov, V. V. Peskov, E. G. Shustin, A. A. Schekin, and V. A. Bykov

Presented by Academician Yu.V. Gulyaev June 16, 2011

Received August 12, 2011

DOI: 10.1134/S1028335812010077

The graphite monolayer, i.e., graphene, recently separated in a free form under normal conditions exhibited unique physical properties of the two-dimensional system containing massless carriers, i.e., Dirac fermions, and high potential application possibilities for developing next-generation field-effect transistors [1], transparent conductive electrodes [2], and others. The first graphene samples produced by mechanical splitting from graphite were characterized by lateral sizes on the order of several micrometers and could be used only for laboratory studies. Practical implementation of graphene-based nanostructures in electronics and optoelectronics raised the problem of high-quality large-area graphene production.

Recently, significant progress was achieved using chemical vapor deposition (CVD) of graphene onto a Ni substrate followed by its transfer onto an arbitrary substrate [3, 4]. Although the area of continuous graphene films produced in such a way is large, their microscopic thickness variance is significant, from ten graphene layers to one, whereas the lateral sizes of the corresponding domains of one- and two-layer graphene are only $\sim 5 \mu\text{m}$.

We proposed and tested a fabrication technology of monatomic graphite layers (graphene) and other conductive layered materials using low-energy ion etching in a plasma-chemical reactor based on beam-plasma discharge [5].

At the initial stage, thin graphite crystals of thicknesses from hundreds of atomic layers more than $100 \times 100 \mu\text{m}^2$ in area were obtained by splitting natural graphite single crystals using an adhesive tape which

was then placed in acetone. After adhesive tape dissolution in acetone, the remaining thin graphite crystal flake was transferred onto a polycor substrate and subjected to ion etching.

Later on, the method for producing thin graphite crystals was modified.

Currently, thin graphite crystals of thickness from ten to hundreds of atomic layers with lateral sizes from 0.5 mm, being workpieces for subsequent etching, are produced by thinning natural graphite single crystals glued on polycor or glass substrates using an adhesive tape. White Stycast epoxy glue or the NOA61 photopolymer are used. Such a method for preparing samples for etching significantly simplified the arrangement of thin graphite crystals on a substrate. Such a method made it possible to obtain thinner initial graphite crystals, which allowed reducing the etching

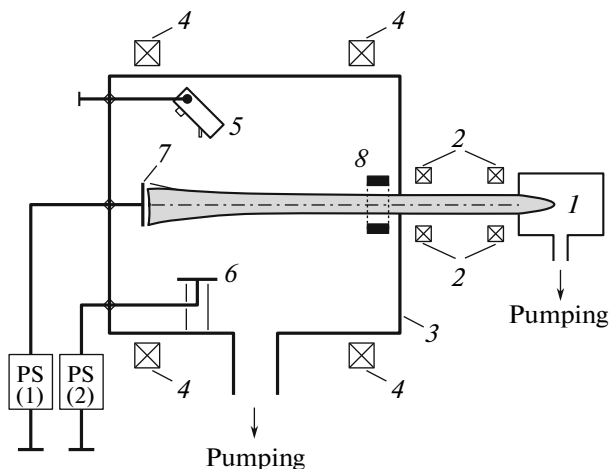


Fig. 1. Schematic diagram of the setup: (1) electron injector, (2) focusing coils, (3) vacuum chamber, (4) Helmholtz coils, (5) ion energy analyzer, (6) substrate holder, (7) discharge collector, (8) control electrode. PS is the power supply unit.

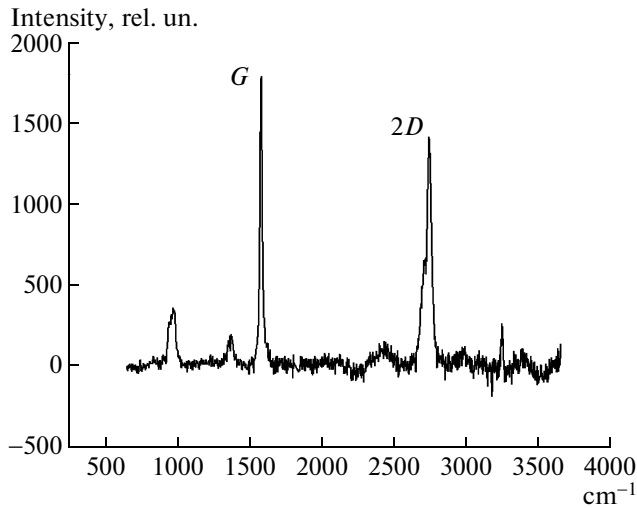


Fig. 2. Local Raman spectrum of the graphite sample after etching.

time and ion energy, thus minimizing the probability of introducing radiation defects.

Then, indium electrodes were applied to sample boundaries, and the crystal was thinned by plasma etching in a beam-plasma reactor in an argon atmosphere. The reactor schematic diagram is shown in Fig. 1. Plasma is generated in a vacuum chamber, i.e., a cylinder of diameter $2R_0 = 0.5$ m and of the same length. An argon working pressure of 0.006–0.2 Pa is maintained in the chamber.

A longitudinal magnetic field of 5 mT in the chamber is induced by Helmholtz coils. The source of the axial electron beam is a Pierce diode gun with a planar hexaboride cathode, placed into an individual chamber connected to the main one by a pressure drop pipe. In the electron gun and drift region before the plasma chamber input, the beam motion is limited by the longitudinal magnetic field $H_d = 10$ mT (selected experimentally by the beam current maximum in a good vacuum). The electron beam parameters at the plasma chamber input are as follows: the accelerating voltage $U_b = 1$ –3 kV, current I_b is to 500 mA, and the characteristic diameter is 1–1.5 cm. The power supply unit provides the gun operation in both continuous and pulsed modes. The pulse duration in the latter case is $\tau_b = 10$ –200 ms.

The film thickness was measured by the in situ resistance in the plasma reactor chamber. The resistance time behavior made it possible to estimate the etch rate and to determine its end time point; the resistance of a square of a homogeneous monolayer is estimated as ~ 2 –3 k Ω .

The argon ion energy was 50 eV at the initial etching stage and decreased to 20 eV at the final stage, as the interelectrode resistance reached $\sim 100 \Omega$.

Graphite films fabricated in such a way were characterized by Raman spectroscopy using an Ntegra Spectra device (NT-MDT Co., Russia). The spectrum is shown in Fig. 2. It contains three lines corresponding to graphene: the relatively weak *D*-line in the range of 1300–1400 cm^{-1} , characterizing the vibrational energy of sp^3 -type C–C bonds, the *G*-line in the range of 1550–1600 cm^{-1} , characterizing the vibrational energy of sp^3 -type C=C bonds, and the *2D* overtone in the region of 2700 cm^{-1} , whose shape allows the estimation of the local number of graphene layers [6]. The ratio of *G*- and *2D*-line amplitudes corresponds to two-layer graphene. The *G*-line narrowness indicates the high quality of the sample. The results of scanning of an area of $74 \times 1.6 \mu\text{m}^2$ with a step of 0.2 μm with complete spectrum acquisition at each point show a uniform contrast of the centroid of the *2D*-line in this region.

Thus, bigraphene samples with characteristic sizes exceeding $100 \times 100 \mu\text{m}^2$ and few layered graphene (FLG) samples with characteristic sizes exceeding $500 \times 500 \mu\text{m}^2$ were fabricated for the first time. High structural quality of the obtained two-layer graphene films and their homogeneity over the sample area were demonstrated.

During graphene production, it was detected that wrinkles, i.e., stable structures shaped as a dihedral angle, are often formed on the crystal surface at the stage of mechanical splitting of natural graphite single crystals using an adhesive tape and are retained after etching to a monolayer. Similar structures spontaneously arise during transverse deformation of a free thin graphite single crystal. They remain stable after stress relief. It can be assumed that they are stabilized by certain dislocation structures; in this case, stresses at the dihedral angle vertex and in the lower region correspond to tension and compression, respectively. In the region of wrinkle edges, modification of planar sp^2 bonds can be expected. Wrinkles on the crystal appear along symmetric crystallographic directions in the basal plane, since their edges are shaped as lines parallel or crossed at an angle of 60° , forming equilateral triangles. The AFM profile of one of the wrinkles is shown in Fig. 3. The wrinkle length can reach several millimeters; the curvature radius in the edge region is from hundreds to several nanometers, depending on the crystal thickness. The wrinkle edge is a very homogeneous quasi-one-dimensional object whose properties can differ from a planar strip of the same crystal due to the edge surface curvature. In a sense, the graphene wrinkle edge can be considered as a part of

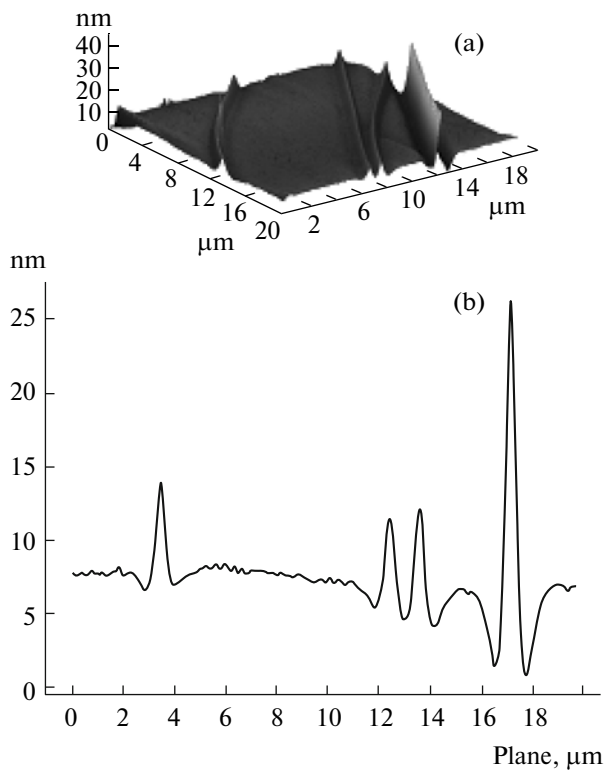


Fig. 3. Wrinkles on the sample surface: (a) atomic-force microscope image and (b) surface section.

an open single-walled nanotube. The curvature in the wrinkle region can result in the formation of local magnetic pseudo-fields [7] which change the carrier spectrum in the wrinkle edge region. All the above points to the wrinkles in thin graphite (graphene) as a new interesting quasi-one-dimensional nanoobject promising for both basic research and applications in graphene-based nanoelectronics.

The single crystals obtained by thinning were also characterized by magnetotransport measurements. Hall-bridge-type structures with a characteristic length between potential contacts of 200–300 μm and a channel width of 20–30 μm were fabricated on crystals by masking and etching in oxygen discharge. Ini-

tial unthinned crystals ~ 100 nm thick at liquid-helium temperatures were characterized by a very high magnetoresistance, $r = R(H=20 \text{ T})/R(H=0) \sim 10^4$ which is comparable to the best bulk graphite single crystals [8] and corresponds to a carrier mobility of $\sim 10^7 \text{ cm}^2/(\text{Vs})$. After thinning to 1 nm, the crystal magnetoresistance decreased by 2–3 orders of magnitude, which allows us to estimate the carrier mobility as $\sim 10^4\text{--}10^5 \text{ cm}^2/(\text{Vs})$. It corresponds to the best graphene samples obtained by mechanical splitting.

Thus, the new direction of nanotechnology fabrication of atomic-thin high-quality graphite films with relatively large lateral sizes using controlled low-energy ion etching of thin natural graphite single crystals is demonstrated.

ACKNOWLEDGMENTS

This study was supported by the Russian Foundation for Basic Research (project nos. 11-02-01379-a, 11-08-00257-a, 11-02-90515-Ukr_f_a, 11-02-12167-ofi-m), state contracts nos. 16.740.11.0146, 16.513.11.3066, and programs of the Russian Academy of Sciences.

REFERENCES

1. K. S. Novoselov, A. K. Geim, and S. V. Morozov, *Science* **306**, 666 (2004).
2. R. R. Nair, P. Blake, and A. N. Grigorenko, *Science* **30**, 1308 (2008).
3. K. S. Kim, Y. Zhao, H. Jang, et al., *Nature* **457**, 706 (2009).
4. A. Reina, X. Jia, and J. Ho, *Nano Lett.* **9**, 30 (2009).
5. E. G. Shustin, N. V. Isaev, M. P. Temiryazeva, and Yu. V. Fedorov, *Vacuum* **83**, 1350 (2009).
6. A. C. Ferrari, J. C. Meyer, V. Scardaci, et al., *Phys. Rev.* **97**, 187401 (2006).
7. F. Guinea, M. I. Katsnelson, and A. K. Geim, *Nat. Phys.* **6**, 30 (2010).
8. Y. Kopelevich, B. Raquet, and M. Goiran, *Phys. Rev. Lett.* **103**, 116802 (2009).

Translated by A. Kazantsev